TJNN Thai Journal of Nanoscience and Nanotechnology

Extraction and Incorporation of Plant-Derived Nanofibrillated Cellulose into Resins for Enhanced Bioplastic Performance

Ilyas Fergo Junaidi[1,3*], Yeo Tze Yuan[1], Sadavut Garagate[3], Sasiwimol Sompruek[3], Teerapat Lapsirivatkul[3], Perameth Suttiruengwong[2,3], Nathithon Chuphandung[4], Rattabun Saengsawat[4], Supakij Suttiruengwong[4,*]

[1]*Chemical Engineering, Food, Chemical and Biotechnology, Singapore Institute of Technology (SIT), Singapore, 828608, Singapore*
[2]*The Demonstration School of Silpakorn University (DSU), 6 Rajamankha Nai Rd, Phra Prathom Chedi Sub-district, Mueang Nakhon Pathom District, Nakhon Pathom, 73000, Thailand*
[3]*Nano Onions Co., Ltd., 25/143 Moo 2, Bang Kaeo Subdistrict, Bang Phli District, Samut Prakan, 10540, Thailand*
[4]*Sustainable Materials Laboratory, Department of Materials Science and Engineering, Faculty of Engineering and Industrial Technology, Silpakorn University, Sanam Chandra Palace Campus, Nakhon Pathom, 73000, Thailand*

Received: 24 March 2026, Revised: 29 June 2026, Accepted: 8 July 2026

Abstract

The development of sustainable reinforcement materials from agricultural waste is essential for advancing biodegradable polymer technologies and circular economy practices. This study investigated the extraction and incorporation of plant-derived nanofibrillated cellulose (NFC) from organic rice straw and bamboo sticks and leaves into a biopolymer resin to enhance its mechanical performance while valorizing agricultural waste. NFC was extracted via chemical pre-treatment and mechanical fibrillation and characterized via FTIR, SEM, TEM, and XRD. The results revealed that NFC derived from organic rice straw exhibited well-defined fibrillar networks, nanoscale diameters, and crystalline features of cellulose that most closely resembled those of commercial NFC, whereas bamboo-derived NFC displayed irregular and poorly fibrillated morphologies. The incorporation of organic rice straw NFC into the resin resulted in modest improvements in tensile strength, elastic modulus, and impact resistance, indicating enhanced stiffness and load transfer, although the variability in mechanical performance highlighted challenges related to NFC dispersion and interfacial bonding. Biodegradability testing under natural composting conditions further demonstrated the progressive degradation of NFC-reinforced resin compared with conventional plastic, confirming the potential of organic rice straw NFC as a sustainable reinforcement material for biodegradable composite applications.

Keywords: Nanocellulose, Bioplastic, Biopolymer, Rice straw, Resin

1. Introduction

Plastic pollution remains among the most pressing global environmental challenges and is driven by the mass production and improper disposal of non-biodegradable petroleum-based plastics that persistently accumulate in marine and terrestrial ecosystems [16, 39]. Conventional petroleum-based plastics, including polyethylene terephthalate (PET), high-density polyethylene (HDPE), polypropylene (PP), and polystyrene (PS), are widely used due to their durability, versatility, and low manufacturing cost; however, their poor biodegradability has created an urgent need for sustainable alternatives, particularly for single-use applications [7].

Biodegradable polymers such as Polylactic acid (PLA), Polyhydroxyalkanoates (PHA), and starch-based biopolymers have been extensively investigated as renewable substitutes for conventional plastics. Nevertheless, their wider application remains limited by inherent drawbacks such as brittleness, moisture sensitivity, and poor impact resistance [15, 26]. Among emerging alternatives, seaweed-derived biopolymer resins offer distinct environmental advantages, as seaweed cultivation requires no arable land and no freshwater irrigation, and characterized by rapid biomass productivity,

Corresponding Author: 2100946@sit.singaporetech.edu.sg and suttiruengwong_s@su.ac.th

making it a highly sustainable feedstock compared to terrestrial bioplastics [3]. However, despite these advantages, seaweed-based biopolymers generally exhibit poor mechanical performance, which remains the primary barrier to commercial adoption [20]. Nano Onions Co. Ltd., a Thailand-based startup, has developed seaweed-based drinking straws derived from *Ulva rigida* as a practical example of this material system, highlighting the need to enhance its mechanical properties [25].

Among the various bio-based reinforcing materials, nanofibrillated cellulose (NFC) has attracted considerable attention due to its biodegradability, renewability, high aspect ratio, large specific surface area, and excellent mechanical properties [13, 19]. NFC is derived from cellulose extracted from plant-based sources such as wood, agricultural residues, and other lignocellulosic biomass through mechanical, chemical, or enzymatic treatments [28]. Compared with other cellulose derivatives, including microcrystalline cellulose (MCC) and nanocrystalline cellulose (NCC), NFC has superior reinforcing capability due to its interconnected nanoscale fibrillar network, which enhances stress transfer efficiency and interfacial adhesion within polymer matrices [35]. While MCC is commonly used as a filler, its micron-scale dimensions limit its uniform dispersion and reinforcement efficiency. In contrast, NFC exhibits a tensile strength of approximately 2 GPa and a Young's modulus of approximately 138 GPa, making it comparable to certain synthetic nanofillers while maintaining biodegradability and renewability [37]. Consequently, NFC has been widely studied as a reinforcing agent in biodegradable polymer composites to improve mechanical performance. However, although NFC reinforcement has been extensively investigated in conventional biodegradable matrices such as PLA and PHA, its application in seaweed-derived biopolymer resin systems remains relatively unexplored [45].

Thailand generates abundant agricultural residues, including organic rice straw and bamboo, which represent underutilized renewable feedstocks for NFC production [14]. To the best of the authors' knowledge, comparative studies evaluating NFC derived from different agricultural waste sources within the same seaweed-based resin system under identical processing conditions remain scarce. This study addresses this gap by extracting NFC from organic rice straw and bamboo using a standardized chemical–mechanical process, incorporating both into the same seaweed-based biopolymer resin, and evaluating their effects on the tensile, flexural, and impact properties of the resulting biocomposites.

2. Experimental

2.1 Material collection and preparation

Organic rice straw was obtained from Farm Ban Rao in Thailand, and bamboo leaves and bamboo sticks were collected from the Silpakorn University Sanam Chandra Palace School compound. All the samples were thoroughly washed with distilled water, dried, and cut into smaller pieces before grinding. Sieving was performed, and samples with particle sizes between 300 µm and 1000 µm were selected for the experiments because they were not overly fine or too coarse [29]. The material collection and preparation procedures are shown in Fig. 1.



Fig. 1. a) Bamboo sticks and leaves collected at Silpakorn University School Compound, b) Organic rice straw from Farm Ban Rao, c) All samples grouded to fine sizes, and d) Sieving was performed with particle sizes between 300 µm and 1000 µm.

2.2 Alkali treatment

All the samples were subjected to alkali treatment to remove lignin. 5% (w/v) sodium hydroxide (NaOH) solution was prepared by dissolving 6 g of NaOH in 120 mL of distilled water and maintaining a 1:12 solid-to-liquid ratio [27, 43]. Ten grams from each sample were added to 120 mL of NaOH solution separately and heated in a water bath at 80 °C for 3 hours with continuous stirring. After treatment, vacuum filtration was performed, and the samples were washed with distilled water until a neutral pH was reached to remove any residual alkali or impurities.

2.3 Bleaching

The organic rice straw, bamboo sticks, and bamboo leaves were bleached to remove additional lignin and hemicellulose [32]. A 4% (w/v) hydrogen peroxide solution was prepared by diluting 16 mL of 30% commercial-grade hydrogen peroxide in distilled water to a final volume of 120 mL. Each sample was added to the bleaching solution, and the mixture was heated at 80 °C with gentle stirring for 2 hours. A visible color change to yellowish white was observed, indicating successful bleaching. The samples were centrifuged for 1 hour at 5000 rpm to remove any remaining liquids by discarding their supernatant. If the samples remained brown, the bleaching process was repeated.

2.4 Acid hydrolysis

Hydrochloric acid (37%) w/v was prepared to remove any cellulose nanocrystals by diluting 12 mL to a final volume of 120 mL with distilled water. The samples were then added with gentle stirring with heat at 50 °C for 1 hour. The samples were then centrifuged for 1 hour at 5000 rpm to separate the solids and were washed multiple times using distilled water to adjust the pH levels to a neutral level [21] as can be seen in Fig. 2.



Fig. 2. Alkali treatment, bleaching, and acid hydrolysis were conducted on all samples to remove lignin and hemicellulose

2.5 Nanofibrillated cellulose (NFC) extraction

NFC was extracted via mechanical fibrillation using ultrasonication. All treated cellulose samples were dispersed in distilled water at a concentration of 1 wt% prior to ultrasonication. Ultrasonication was performed using an Ultrasonic Processor VCX 750 in pulse mode with 5 seconds on and 5 seconds off for a total duration of 30 minutes, delivering a total energy input of approximately 100,000 J [5].

To prevent thermal degradation of the cellulose during sonication, the samples were maintained in an ice bath throughout the process, as shown in Fig. 3. Following ultrasonication, the suspensions were then centrifuged at 5000 rpm for 30 minutes to remove larger fibril aggregates. The supernatants containing the NFC-rich fraction were then collected.

These supernatants, also known as NFC suspensions, were freeze-dried (Fig. 4) under reduced pressure at -20 °C overnight to obtain dry NFC powder for subsequent steps of characterization and incorporation into biopolymer resins.



Fig. 3. Ultrasonication of samples to separate fibrils of NFC

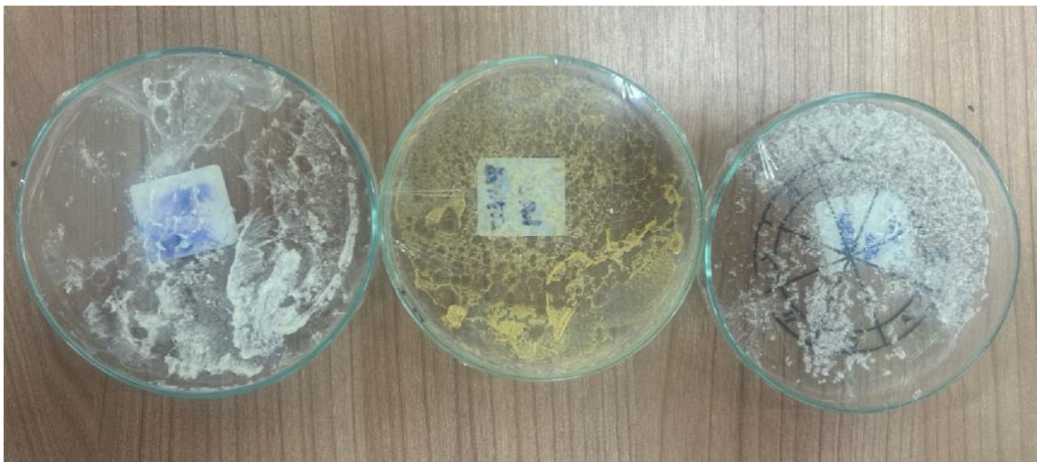


Fig. 4. Post freeze drying of NFC powder samples

2.6 Incorporation of nanofibrillated cellulose (NFC) into polymer resin via melt compounding

Two resin formulations were prepared in this study to evaluate the effect of organic rice straw NFC on the mechanical performance of Nano Onions biopolymer resin. Bamboo sticks and leaves were not selected since organic rice straw showed more promising morphological results. The formulations were designed to allow direct comparison in mechanical performance between NFC reinforcement and ground *Ulva rigida* seaweed as alternative bio-based reinforcement materials. The Nano Onions proprietary resin used in this study include biopolymers such as polyhydroxy acid (PLA) and polybutylene succinate (PBS), forming the base matrix for NFC incorporation.

Batch 1 consisted of Nano Onions resin reinforced with organic rice straw NFC, without the addition of grinded *Ulva rigida* seaweed. The base resin mass weighed at 88.2 g, and NFC was incorporated at a loading value of 2 phr (2 wt%), corresponding to 1.8 g, resulting in a total batch mass of 90 g.

Batch 2 consisted of Nano Onions resin reinforced with grinded *Ulva rigida* seaweed, without the incorporation of organic rice straw NFC. Similarly, 88.2 g of Nano Onions resin was used, and grinded *Ulva rigida* seaweed was added at 2 phr (2 wt%), corresponding to 1.8 g, giving a total batch mass of 90 g. The NFC loading of 2 phr (2 wt%) was selected following the optimal mechanical reinforcement of biopolymer matrices using plant-derived NFC, which commonly occurs at low loading

levels in the range of 1–3 wt%, while higher loadings may lead to filler agglomeration and deterioration of mechanical properties [43].

Before internal mixing, both batches were oven-dried at 80 °C for 24 h to remove residual moisture, thereby preventing moisture-induced processing defects, reducing hydrolytic degradation during melt processing, and promoting uniform dispersion in the internal mixer [18].

MX105-D40L50 internal mixer (Charoen Tut Co. Ltd.) was used for the melt compounding process for both batches. The mixing chamber temperature was set to 180 °C, and the rotor speed was maintained at 65 rpm. For each batch, the resin and corresponding reinforcement material (NFC or grinded ulva rigida) were fed into the internal mixer and compounded for a total mixing duration of 10 minutes to promote uniform filler dispersion within the polymer matrix. Subsequently, both batches were then subsequently size-reduced using a granulator to obtain uniformly sized granules before compression molding as can be seen in Fig. 5.



Fig. 5. Diagram flow of melt compounding to the grinding of resin mix before compression

2.7 Compression molding of NFC–resin composite into mechanical test specimens

A compression molding process was then used for the ground resins from the internal mixer to be molded into appropriate sizes for mechanical testing. Dog-bone molds in accordance with ASTM D638 Type V standard were used for tensile testing and rectangular molds in accordance with ASTM D256 were used for impact testing. Before molding, both composite batches were oven-dried at 80 °C for 24 hours to remove residual moisture and minimize the risk of void formation during compression. This secondary drying step ensured consistent material behaviour during molding [41].

A compression molding press machine (Charoen Tut Co. Ltd.) was used. The upper and lower plates, together with the molding plates, were preheated to 190 °C for 5 minutes prior to ensuring uniform thermal conditions before sample loading. The dried composite materials from both batches were then placed into the respective mold cavities and filled to the required volume to achieve uniform specimen thickness. Compression molding was subsequently carried out at 190 °C for 5 minutes, followed by cooling for 5 minutes to allow solidification of the molded specimens. After cooling, the molds were opened, and the specimens were carefully removed. The resulting specimens were composed of dog-bone tensile strength samples and rectangular impact test samples for both composite batches. These specimens were subsequently used for tensile and impact testing, as shown in Fig. 6.



Fig. 6. Diagram flow of compression molding of resin to tensile and impact test specimens

2.8 Characterization

ATR-FTIR spectra of the samples were recorded to identify the functional groups present in the cellulose at each stage of extraction. Spectra were collected using an ATR-FTIR spectrophotometer (Bruker, model Alpha II, Bruker Optics, Germany) at room temperature from 4000 to 500 cm^{-1} using a nominal resolution of 4 cm^{-1} and 16 scans.

XRD patterns of the EC were collected via X-ray diffractometer (XRD-6100, Shimadzu, Japan) with Cu-Kα radiation (λ = 0.1541 nm) over a scanning 2θ range of 10–50°.

The morphology of the composites was examined using a TESCAN MIRA3 LMH Schottky field emission scanning electron microscope (FE-SEM) operated at an accelerating voltage of 5 kV. Before imaging, the samples were cross-sectioned and sputter-coated with gold-palladium.

The morphology, size, and structural features of the synthesized CDs were examined using field emission transmission electron microscopy (FETEM). Imaging was conducted on a JEOL JEM-3100F (JEOL, Japan) instrument operating at an accelerating voltage of 200 kV.

The mechanical performance of the films was evaluated using UTM (NRI TS500-5B) following ASTM D638 Type V standard. Izod impact testing was performed following ASTM D256. Before testing, all specimens were notched at the midpoint to ensure controlled crack initiation during impact. Impact testing was conducted using an Instron CEAST 9050 Impact Pendulum, following the notched Izod configuration specified in ASTM D256 and using a 5 J pendulum hammer, commonly used for thin polymer specimens.

3. Result and discussion

3.1.1 ATR-FTIR of before and after plant-derived NFC extraction

ATR_FTIR spectroscopy was conducted to evaluate the chemical structural changes of the plant-based feedstocks before and after NFC extraction. These FTIR spectra results are shown in Figures 7,8,9. The results showed that the spectra obtained from bamboo sticks, bamboo leaves, and organic rice straw before performing NFC extraction exhibited characteristic absorption bands associated with cellulose, hemicellulose, and lignin, confirming the lignocellulosic nature of the raw biomass. Before NFC extraction, all raw samples showed a distinct absorption band around 1730 cm^{-1}, which is attributed to the C=O stretching vibration of acetyl and uronic ester groups in hemicellulose, as well as ester linkages between lignin and carbohydrates. In addition, prominent peaks near 1500–1515 cm^{-1} were observed, corresponding to aromatic skeletal vibrations of lignin. These peaks are commonly reported in untreated lignocellulosic materials and indicate the presence of noncellulosic components such as lignin and hemicellulose [2, 23].

After conducting NFC extraction, significant reductions of the 1730 cm^{-1} carbonyl band and the aromatic lignin peaks around 1500 cm^{-1} were observed across all samples. This confirms the effective removal of hemicellulose and lignin during the chemical pretreatment and ultrasonication processes. Similar literature article. have been reported for NFC extracted from agricultural residues, including rice straw and bamboo, where alkali and bleaching treatments selectively remove amorphous components while preserving the cellulose backbone [11]. This observation is consistent with previous studies, where the disappearance or marked reduction of the bands at approximately 1730 cm^{-1} and 1500 cm^{-1} was attributed to the removal of hemicellulose and lignin during nanocellulose extraction processes [17, 33].

Fig. 7, Fig. 8 and Fig. 9 showed that the ATR-FTIR spectrum after NFC extraction retained the characteristic cellulose absorption bands at ~3335 cm^{-1}, ~2895 cm^{-1}, and ~1030 cm^{-1}. The broad band around 3335 cm^{-1} corresponds to O–H stretching vibrations, reflecting the hydrogen-bonded hydroxyl groups of cellulose. The peak at 2895 cm^{-1} is attributed to C–H stretching vibrations of aliphatic methylene groups, while the strong band near 1030 cm^{-1} is associated with C–O–C and C–O stretching vibrations of the pyranose ring structure of cellulose. The preservation and relative intensification of these peaks after NFC extraction indicate that the cellulose crystalline structure was successfully retained, which is in agreement with previous studies reporting that nanocellulose extraction removes non-cellulosic components while maintaining the characteristic cellulose functional groups and backbone structure[6, 17]. Thus, the ATR-FTIR results confirm the successful extraction of NFC from

all the raw samples by the effective removal of lignin and hemicellulose while retaining the fundamental cellulose chemical structure.

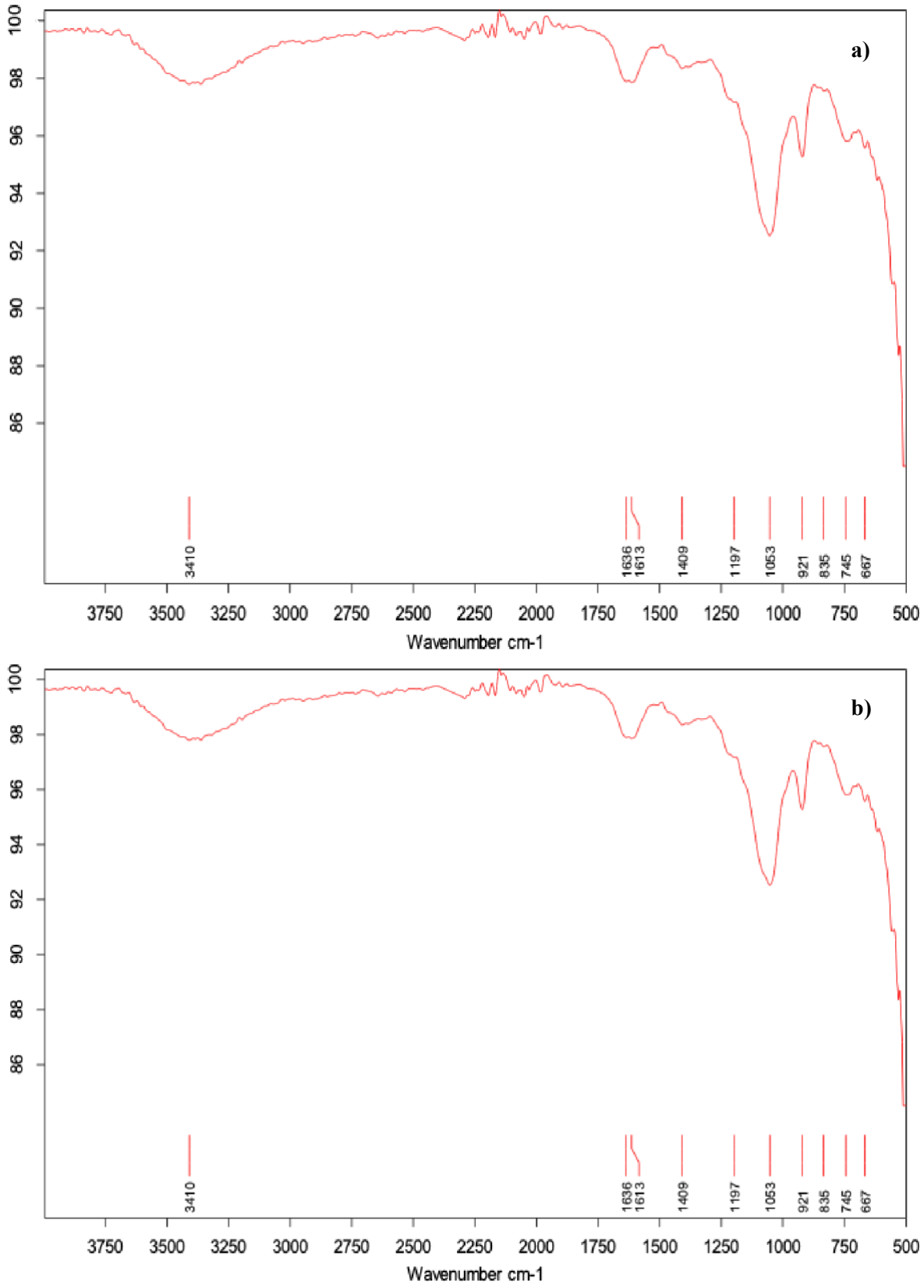


Fig. 7. ATR-FTIR spectra of before a) and after b) NFC extraction of bamboo leaves

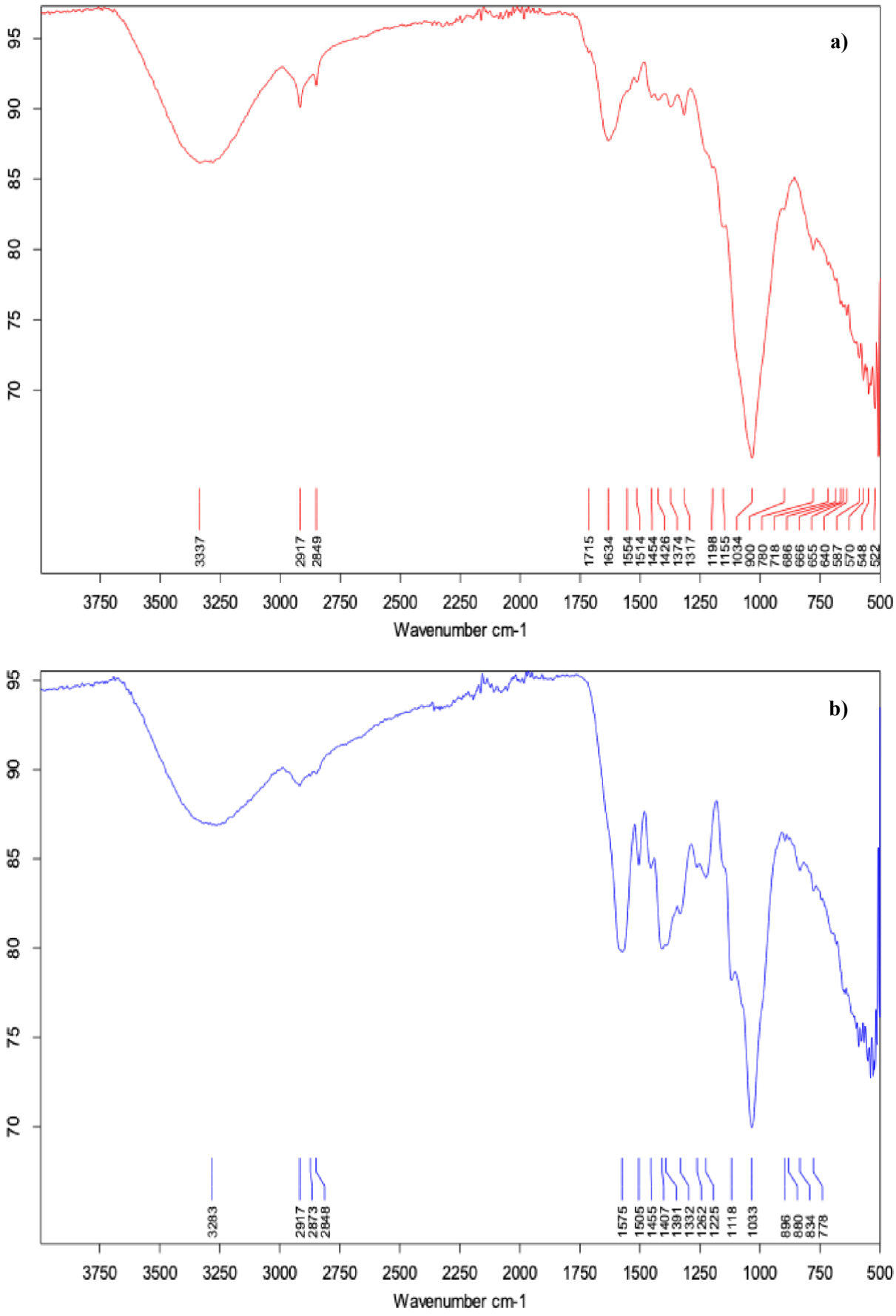


Fig. 8. ATR-FTIR spectra of before a) and after b) NFC extraction of bamboo sticks

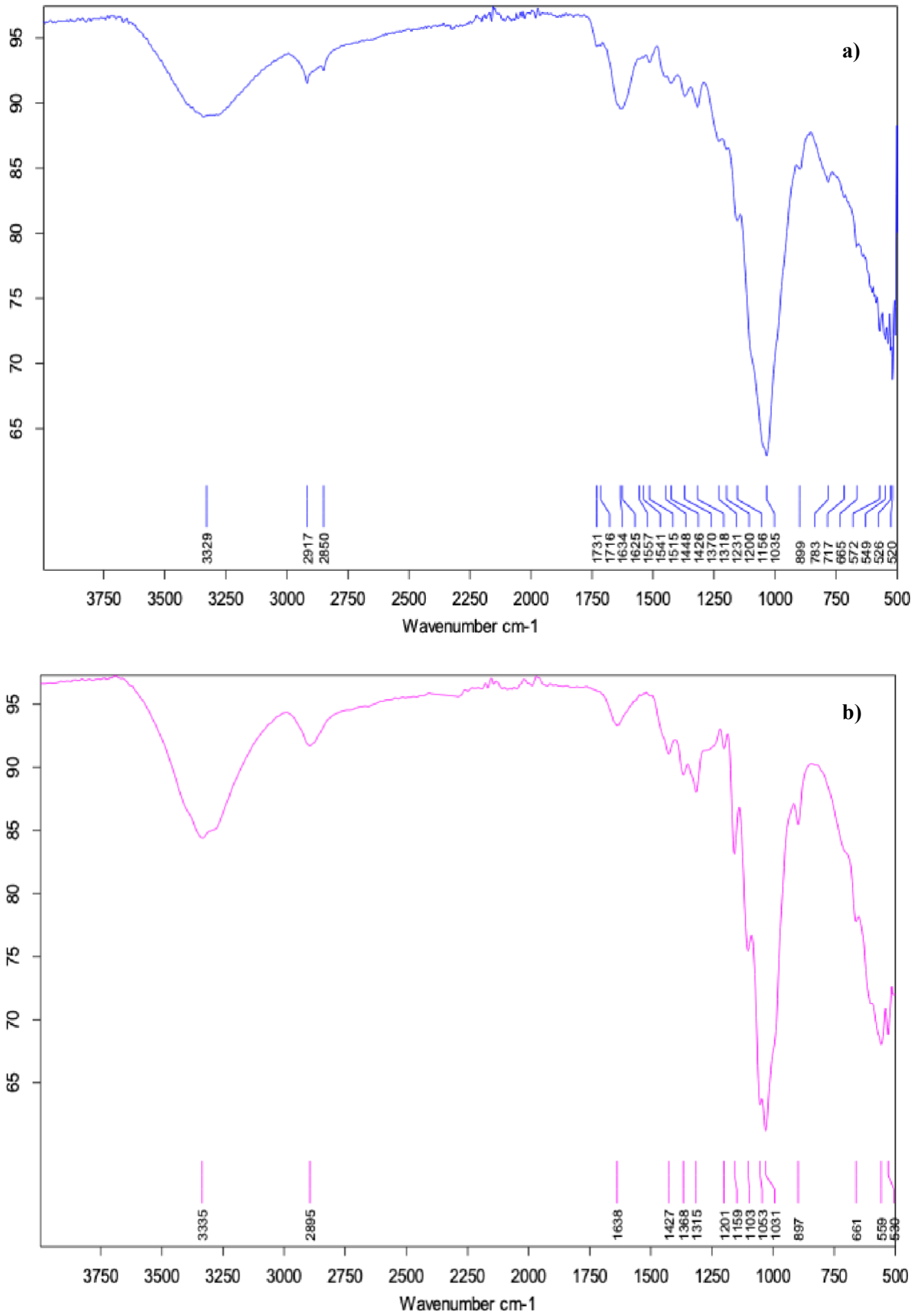


Fig. 9. ATR-FTIR spectra of before a) and after b) NFC extraction of organic rice straw

3.1.2 ATR-FTIR comparison of samples with commercial NFC

ATR-FTIR analysis was subsequently conducted to compare the functional groups and chemical compositions of the plant-derived NFCs with a commercial NFC. In Fig. 10, the organic rice straw NFC shows the highest spectral similarity to the commercial NFC in terms of peak position, band shape, and relative intensity.

A broad O-H stretching band is observed at approximately 3440 cm^{-1} for both organic rice straw NFC and commercial NFC, corresponding to hydroxyl groups involved in intermolecular and intramolecular hydrogen bonding within the cellulose structure [34]. The close overlap of this band suggests comparable hydrogen-bonding networks and cellulose purity. This observation is consistent with previous studies on rice-husk-derived nanocellulose, where a prominent O-H stretching band around 3340–3450 cm^{-1} was attributed to the cellulose hydrogen-bonding network and was retained after nanocellulose extraction[9, 33]. In contrast, bamboo sticks and leaves NFCs exhibit broader and less well-defined O-H bands, indicating residual non-cellulosic components.

Most notably, the strong absorption band at approximately 1060 cm^{-1}, attributed to C-O stretching of the cellulose backbone (β-1,4-glycosidic linkages), shows close alignment between organic rice straw NFC and commercial NFC. This band is a key indicator of cellulose integrity, and the similarity in both peak position and intensity indicates that the chemical structure of cellulose in organic rice straw NFC closely resembles that of commercial NFC [36]. Moreover, bamboo sticks and bamboo leaves NFCs displayed noticeable deviations in this region, likely due to residual hemicellulose or lignin-related contributions.

In summary, the ATR-FTIR results demonstrate that organic rice straw NFC exhibits the closest spectral correspondence to commercial NFC, particularly at the O–H stretching (~3440 cm^{-1}), C–H stretching (~2899 cm^{-1}), and C–O stretching (~1060 cm^{-1}) regions. This indicates a higher degree of cellulose purity and structural similarity, supporting the suitability of organic rice straw as a promising agricultural waste for producing NFC as compared to bamboo sticks and leaves. These findings are in good agreement with previous studies on rice-husk-derived nanocellulose, which reported the preservation of characteristic cellulose absorption bands and the successful removal of non-cellulosic components after extraction processes [9, 17, 33].

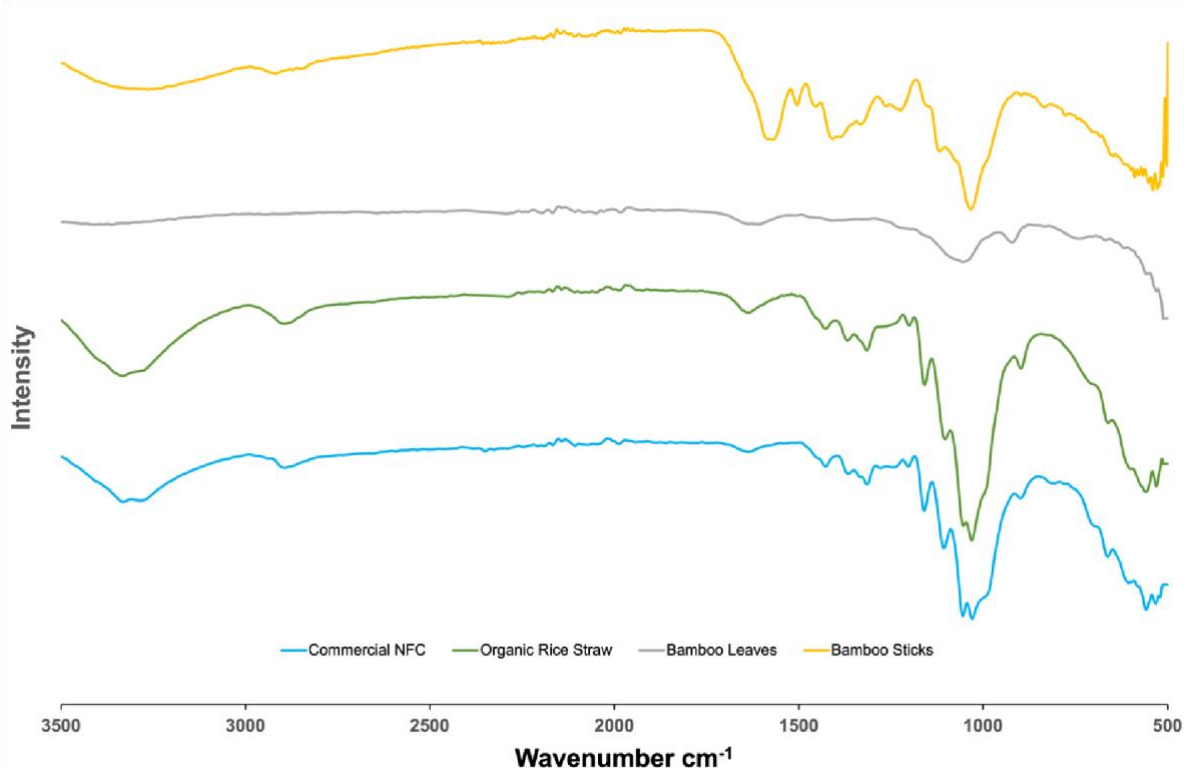


Fig. 10. ATR-FTIR spectra of NFC of samples with a commercial NFC

3.2 Scanning Electron Microscopy (SEM) of samples

The surface morphology and fibrillar structure of the extracted NFCs from organic rice straw, bamboo leaves, and bamboo sticks were examined using Scanning Electron Microscopy (SEM). The SEM images in Fig.11 provide qualitative evidence of fibrillation efficiency and structural integrity following the NFC extraction process.

AS shown in Fig. 11 a), organic rice straw NFC exhibits a well-developed, interconnected fibrillar network consisting of long, entangled cellulose fibrils. The fibrils are clearly distinguishable and exhibit lengths extending to at least ~5 µm, with an average diameter of 36.16 ± 9 nm (n = 50), confirming they were in the nanoscale range. Organic rice straw NFC has been reported to form long, web-like fibrillar networks, with fibril lengths exceeding 5 µm and diameters below 50 nm, closely resembling the morphology observed in this study [12, 24].

In contrast, bamboo leaves and bamboo sticks NFCs samples display irregular, non-uniform, and largely non-fibrillar morphologies. The SEM images reveal collapsed structures, agglomerated regions, and sheet-like fragments rather than discrete nanofibrils as compared to organic rice straw NFC. These features suggest incomplete fibrillation, potentially due to higher residual lignin content or insufficient mechanical disintegration during processing.

Thus, the SEM results demonstrated that organic rice straw NFC exhibits the most well-defined fibrillar morphology, closely matching the fibril length, diameter, and network structure reported for NFC in other literatures. Based on its fibrillation quality and structural resemblance of NFC, organic rice straw was selected for subsequent testing and optimization in NFC extraction and reinforcement with Nano Onions resin.

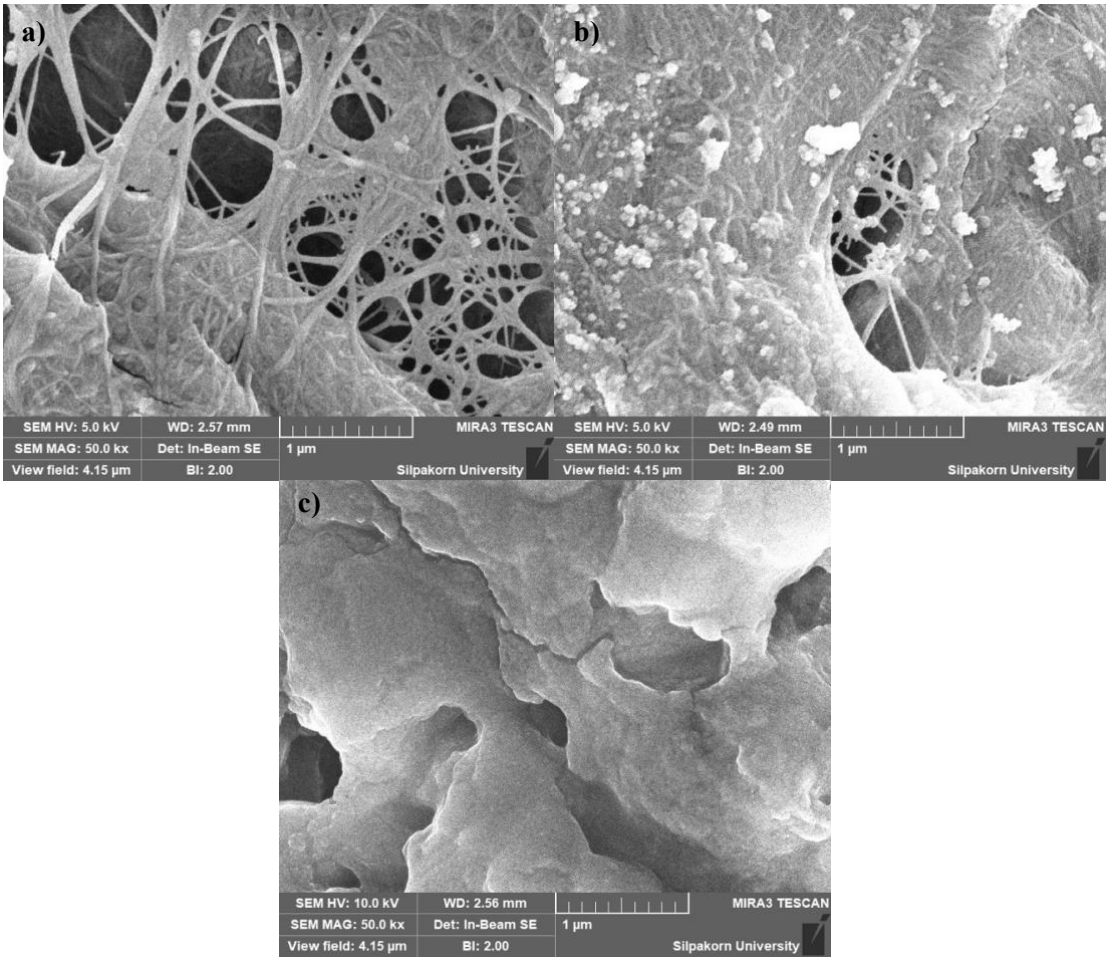


Fig. 11. SEM of a) organic rice straw NFC, b) bamboo leaves NFC, c) bamboo sticks NFC

3.3 X-ray diffraction (XRD) comparison of organic rice straw NFC with a commercial NFC

The crystalline structures of the cellulose in raw organic rice straw, organic rice straw NFC, and commercial NFC were evaluated using X-ray diffraction (XRD). Both organic rice straw NFC and commercial NFC exhibited characteristic diffraction peaks associated with cellulose I, as shown in Fig. 12, indicating that the native cellulose crystalline structure was retained after the extraction of the NFC process. The diffraction peak observed at approximately $2\theta = 16°$ corresponds to the (1–10) and (110) crystalline planes of cellulose I. This peak is commonly attributed to the ordered cellulose regions and is consistently reported in cellulose and NFC studies [8].

The dominant diffraction peak located at approximately $2\theta = 22°$ represents the (200) plane of cellulose I and is considered the main crystalline reflection of cellulose. The presence of this peak in both samples confirms successful isolation of cellulose-rich material. The higher intensity and sharper nature of the 22° peak observed in commercial NFC suggest a higher degree of crystallinity compared to organic rice straw NFC, which is consistent with commercial materials typically undergoing more intensive purification and fibrillation processes [42].

A distinct peak at approximately $2\theta = 38°$ is observed in the raw organic rice straw sample and is attributed to the presence of silica (SiO_2), a well-documented inorganic component naturally abundant in rice straw. Rice plants are known to accumulate silica in their cell walls, and residual silica is commonly detected in XRD patterns of rice straw-derived cellulose, even after chemical treatments [34]. The reduced intensity of this peak in the NFC sample compared to raw rice straw indicates partial removal of inorganic components during the extraction process. Overall, the lower diffraction intensity of organic rice straw NFC relative to commercial NFC suggests a lower crystallinity index, which may be attributed to incomplete removal of amorphous regions or less extensive mechanical fibrillation.

The XRD analysis confirmed that organic rice straw NFC retains the characteristic cellulose I crystalline structure while exhibiting slightly lower crystallinity compared to commercial NFC. The results validate the effectiveness of the extraction process while highlighting the influence of agricultural waste source and processing intensity on cellulose crystallinity.

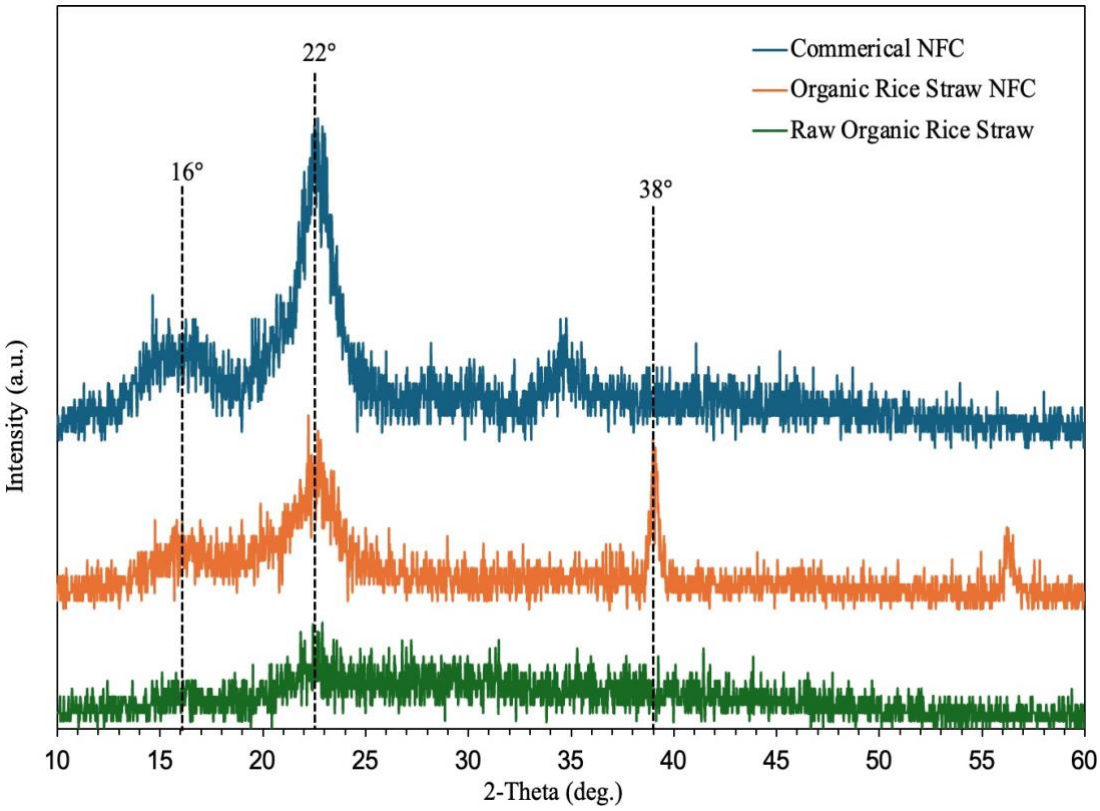


Fig. 12. XRD patterns of raw organic rice straw, organic rice straw NFC, and commercial NFC

3.4 Transmission Electron Microscopy (TEM) of organic rice straw NFC

The nanoscale morphology of organic rice straw NFC is shown in Fig. 13 a) and b), respectively. The organic rice straw NFC in the images showed randomly distributed nanoscale clumps that formed dense and a homogeneous network. Individual fibrils are not visible and this morphology is common in unstained nanocellulose samples derived from agricultural residues which often retain a complex matrix of hemicellulose that facilitates inter-fibrillar bridging [22]. The absence of large rod-like particles or crystalline bundles suggests that the cellulose was successfully fibrillated rather than fragmented into cellulose nanocrystals (CNCs).

Slightly darker regions are shown in Fig. 13, and TEM images were selected for dimensional analysis using ImageJ. The measured domains had an average size of 10.01 ± 1.63 nm(n = 50), indicating that these regions were within the nanoscale range and that certain areas in the images may be attributed to localized fibril overlap or minor aggregation, which is commonly reported in TEM analysis of NFC due to drying effects during sample preparation and strong interfibrillar hydrogen bonding [40].

Overall, the TEM results confirm nanoscale cellulose formation, although extensive aggregation and imaging limitations hindered the clear identification of discrete nanofibrils.

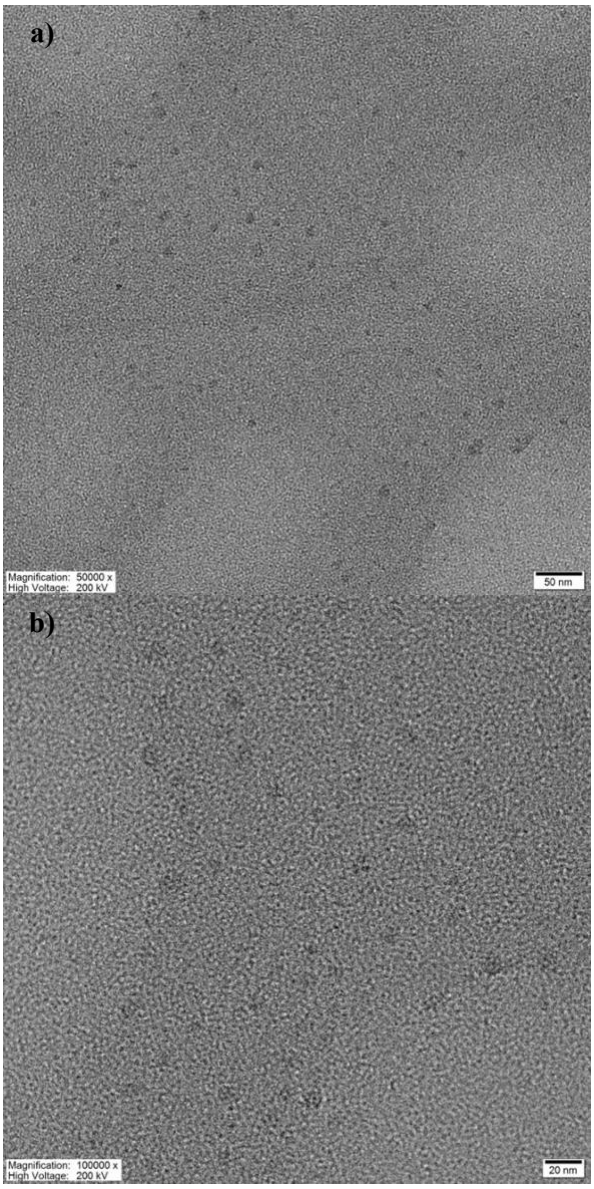


Fig. 13. TEM images of organic rice straw NFC under the scale of a) 50 nm., and b) 20 nm.

3.5 Tensile strength test of organic rice straw NFC-resin specimens

Tensile testing was conducted using a Universal Testing Machine (NRI TS500-5B) following ASTM D638 Type V standard to evaluate the effect of organic rice straw NFC incorporation on the Nano Onions resin in comparison with pure Nano Onions resin without any NFC [1]. For each formulation, five specimens were tested to ensure reproducibility and statistical reliability. Stress–strain curves were recorded, and key mechanical properties including elastic modulus, tensile strength, and elongation at break were determined.

Fig. 14 a) and b) represent the stress–strain behaviour of pure Nano Onions resin and the resin reinforced with organic rice straw NFC, respectively. The NFC-incorporated resin exhibited a slight increase in tensile strength compared to the pure resin. The average tensile strength increased from 16.93 MPa of the pure resin to 17.80 MPa after the incorporation of organic rice straw NFC. This improvement suggests that the presence of NFC contributes to enhanced load transfer within the biopolymer matrix. Similar trends are reported in other studies where rice straw NFC improved tensile strength and Young's modulus in poly(ε-caprolactone) composites, although excessive NFC content can lead to aggregation and reduced performance [30].

Additionally, the elastic modulus increased from an average value of 295.21 MPa for the pure resin to 304.47 MPa for the NFC-incorporated resin, indicating an increase in material stiffness. The elongation at break showed a marginal increase from 8.43% to 8.66% following NFC incorporation, suggesting that stiffness enhancement was achieved without significant loss of ductility. This indicates that NFC reinforcement did not induce embrittlement of the resin at the loading level used.

However, the NFC-incorporated samples exhibited higher data variability, particularly in elastic modulus values, as reflected by the larger standard deviation. This variability is likely due to inconsistent dispersion of NFC within the resin matrix during the incorporation process, which can lead to localized stress concentrations and inconsistent interfacial bonding.

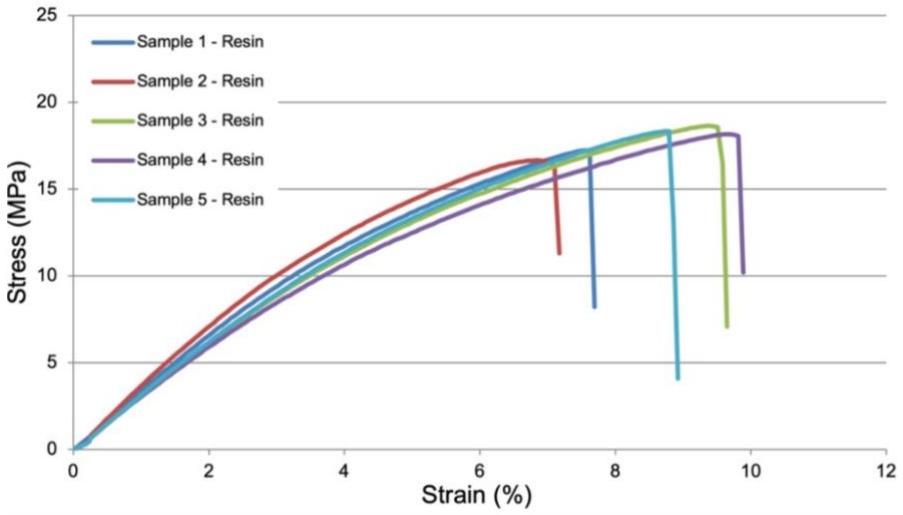
The tensile test results demonstrated that organic rice straw NFC can function as an effective reinforcing agent by enhancing stiffness and tensile strength of the resin. Nevertheless, the mechanical performance is strongly dependent on NFC dispersion quality and interfacial adhesion between the NFC and polymer matrix. Further optimisation of NFC surface compatibility and processing conditions may lead to more consistent mechanical improvements.

3.6 Impact test of organic rice straw NFC-resin specimens

Impact testing was conducted to evaluate the toughness and resistance to sudden loading of the Nano Onions resin with and without organic rice straw NFC. Impact resistance is a critical property for materials intended for packaging and automotive applications, where components may be subjected to accidental drops or sudden impacts [38]. Two batches of samples, similar to those in the tensile strength testing, were prepared for comparison: pure Nano Onions resin and organic rice straw NFC–reinforced resin. Molded rectangular specimens were prepared in accordance with ASTM D256 standards [10]. Before testing, all specimens were notched at the midpoint to ensure controlled crack initiation during impact. Impact testing was conducted using an Instron CEAST 9050 Impact Pendulum, following the notched Izod configuration specified in ASTM D256 and using a 5 J pendulum hammer that is commonly used for thin polymer specimens. For each formulation, five specimens were tested to assess repeatability and variability in impact behaviour.

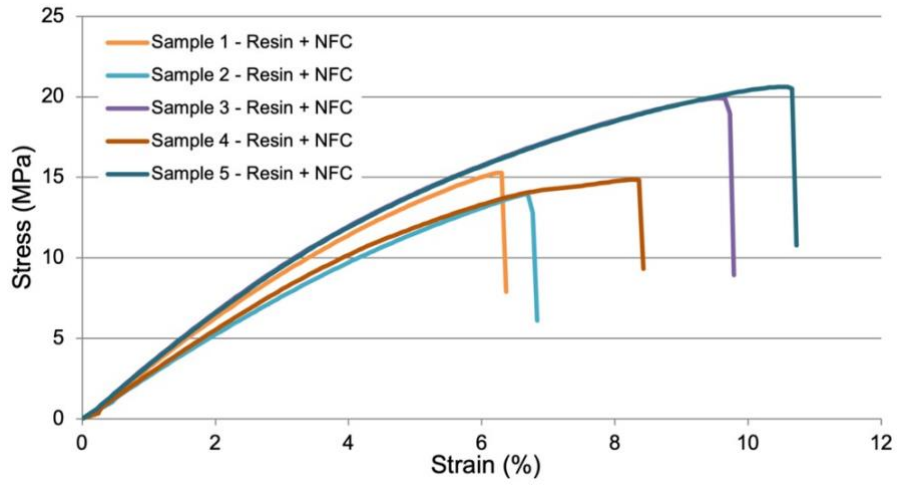
Fig. 15 a) and b) presents the impact energy absorption values of the pure resin and NFC-incorporated resin. The pure Nano Onions resin exhibited relatively consistent impact resistance, with values ranging from 1.14 to 1.64 kJ/m², indicating stable energy absorption behaviour. In contrast, the NFC incorporated resin showed high variability, with impact resistance values ranging from 0.82 to 2.40 kJ/m². While certain NFC-reinforced specimens demonstrated improved impact resistance, others exhibited lower values than the pure resin. This variability suggests that the impact performance of NFC-incorporated resin is highly sensitive to NFC dispersion and interfacial interactions within the polymer matrix. Poor dispersion or NFC agglomeration can act as stress concentration sites, facilitating crack initiation and propagation under impact loading. These findings align with broader research showing that rice straw-based composites can achieve high impact resistance when well-processed, but performance depends heavily on fibre treatment and distribution [4, 38].

a)



Sample number	Modulus (MPa)	Tensile strength (MPa)	Elongation at break (%)
1	304.12	15.29	6.36
2	263.40	13.96	6.83
3	322.54	19.93	9.79
4	260.51	14.86	8.43
5	325.48	20.63	10.73
Average	295.21	16.93	8.43
Standard Deviation	31.46	3.10	1.87

b)



Sample number	Modulus (MPa)	Tensile strength (MPa)	Elongation at break (%)
1	332.47	17.23	7.69
2	346.96	16.65	7.17
3	287.67	18.63	9.64
4	256.12	18.15	9.89
5	299.14	18.33	8.92
Average	304.47	17.80	8.66
Standard Deviation	36.19	0.83	1.19

Fig. 14. a) Tensile test of NFC-resin following ASTM D638, and b)Tensile strength test of pure resin following ASTM D638

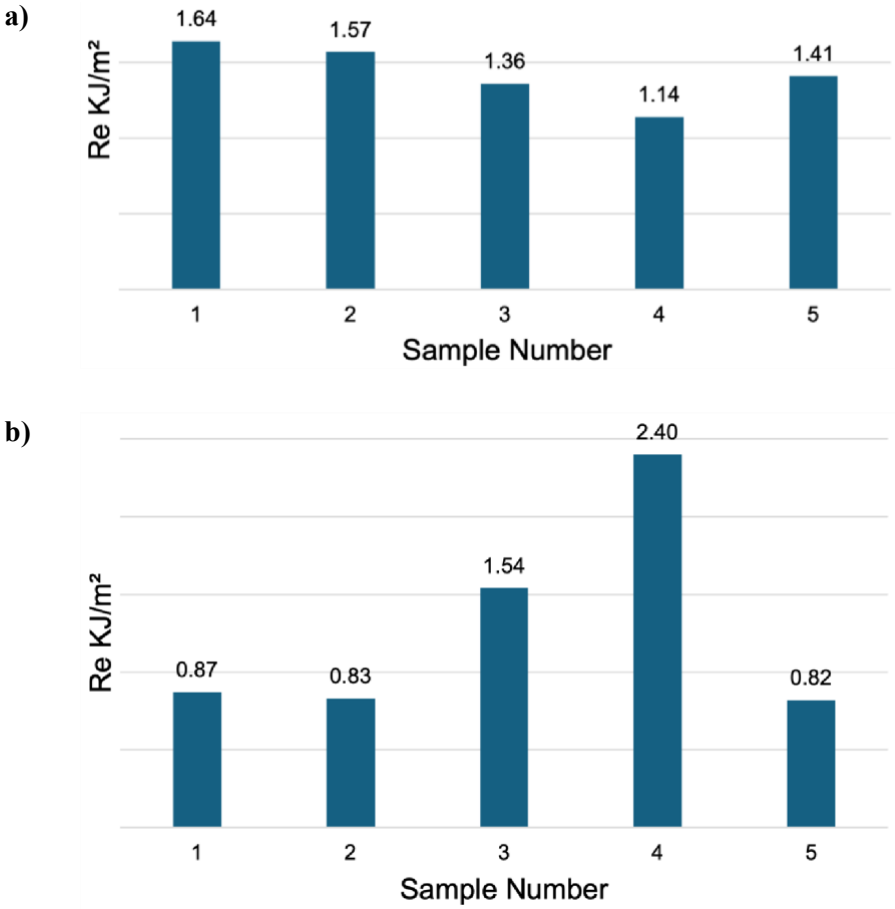


Fig. 15. Impact test of a) NFC-resin, and b) pure resin following Izod ASTM D256

The results from the impact testing indicated that although organic rice straw NFC has the potential to improve impact resistance, consistent toughness enhancement is not guaranteed without uniform NFC dispersion and strong interfacial bonding with the polymer matrix. These findings highlight the importance of optimising NFC processing and dispersion techniques to achieve reliable impact performance in NFC-reinforced biopolymer systems.

3.7 Biodegradability testing of organic rice straw NFC incorporated resin

Biodegradability testing was conducted to evaluate the environmental degradation behaviour of the organic rice straw NFC incorporated into Nano Onions resin under natural composting conditions. To simulate a realistic end-use product, the NFC-reinforced resin was fabricated into a compostable straw, which was then compared against a commercial plastic straw over a period of approximately six months.

Both straws are buried in a 5 kg gunny sack of compost soil with a starting temperature of 64 °C. that indicates good microbial activity. The test was carried out under natural composting settings, where samples were exposed to ambient environmental conditions, microbial activity, and temperature fluctuations typical of composting environments. Visual inspections and photographic documentation were performed periodically to monitor physical degradation, fragmentation, and surface deterioration.

As shown in Fig. 16, the organic rice straw NFC–reinforced straw exhibited progressive degradation over time. During the early stages of composting (Day 1 to Day 9), the straw largely retained its original shape, indicating initial resistance to degradation despite exposure to elevated temperatures. From Day 24 to Day 55, visible signs of deterioration were observed, including surface roughening, discoloration, and partial fragmentation, suggesting the onset of microbial and hydrolytic degradation mechanisms.

At later stages of composting from day 72 to day 143, the NFC-incorporated straw showed significant structural breakdown, with noticeable fragmentation into smaller pieces and loss of

mechanical integrity. This progressive disintegration indicates that the incorporation of organic rice straw NFC enhances the susceptibility of the resin to biodegradation, likely due to the hydrophilic nature of cellulose, which promotes moisture uptake and microbial colonisation within the polymer matrix [44].

In contrast, the commercial plastic straw demonstrated minimal visible degradation throughout the same composting period, maintaining its structural integrity even after extended exposure. This highlights the inherent resistance of conventional petroleum-based plastics to biodegradation under natural composting conditions. The biodegradability test demonstrates that the observed progressive breakdown over six months under natural conditions confirms the material's enhanced environmental compatibility



.

Fig. 16. Biodegradability test of organic rice straw NFC compared to commercial straw

4. Conclusion

4.1 Key findings

This study set out to extract and incorporate plant-derived nanofibrillated cellulose (NFC) from agricultural waste, specifically organic rice straw and bamboo leaves and bamboo sticks, into a biopolymer resin in order to enhance mechanical performance while valorising agricultural waste. Overall, the findings demonstrate that the study successfully achieved its objective as organic rice straw was identified as a more suitable NFC source than bamboo sticks and leaves through characterisation and morphological testing.

The NFC extraction and characterisation results showed that organic rice straw yielded NFC with a more defined fibrillar morphology than bamboo sticks and bamboo leaves, as observed through SEM, as well as FTIR comparison with a commercial NFC. Based on the SEM images, distinct and interconnected fibrils with micrometre-scale lengths consistent with values reported in the literature were observed, indicating effective fibrillation and cellulose isolation. From the FTIR results, organic rice straw showed the most similar peaks to a commercial NFC than bamboo sticks and leaves. These observations guided the selection of organic rice straw as the preferred agricultural waste for subsequent NFC incorporation and performance testing. Mechanical testing demonstrated that incorporation of organic rice straw NFC into the Nano Onions resin resulted in measurable improvements in material performance. Tensile strength testing showed a slight increase in tensile strength and elastic modulus compared to the pure resin, indicating enhanced stiffness and improved load transfer within the polymer matrix. These results confirm that NFC can act as an effective reinforcing filler at low loading levels. However, increased variability in tensile data suggests that NFC dispersion within the resin was not fully consistent. Impact testing also revealed highly variable toughness behaviour for NFC-reinforced specimens. While certain samples showed improved impact resistance, others exhibited reduced values compared to the pure resin. Similarly, this variability highlights the sensitivity of impact performance to NFC agglomeration, dispersion quality, and interfacial bonding, which play a critical role in energy dissipation during sudden loading. The biodegradability assessment over 6 months also demonstrated that the organic rice straw NFC incorporated resin exhibited significantly improved environmental degradability compared to a commercial plastic straw under natural composting conditions. This confirms that the incorporation of plant-derived NFC contributes not only to mechanical reinforcement but also to enhanced compostability, supporting the sustainability objective of this study.

4.2 Future research

The NFC extraction yield achieved in this study was approximately 20%, based on an initial 10 g of raw organic rice straw, bamboo stick and bamboo leaves accordingly. Although this yield is comparable to values reported for mechanically or chemically treated lignocellulosic biomass, it indicates that a significant fraction of cellulose may remain unutilised or lost during processing [31]. Future research should therefore explore alternative NFC extraction methods such as TEMPO-mediated oxidation, which has been widely reported to produce higher NFC yields, more uniform fibril diameters, and improved dispersion stability. TEMPO-oxidised NFC typically exhibits narrower diameter distributions and enhanced surface charge, which can significantly improve fibrillation efficiency and interfacial bonding with polymer matrices.

Additionally, future research should investigate other agricultural waste feedstocks that may offer higher cellulose content, lower lignin levels, or reduced silica content. Potential candidates include sugarcane bagasse, oil palm empty fruit bunches, wheat straw, and corn stover. Comparative studies across different biomass sources would enable identification of feedstocks that provide higher NFC yield, improved fibril quality, and lower processing complexity.

From a composite processing perspective, the inconsistencies observed in tensile, and impact properties suggest that NFC dispersion remains a key challenge. Future work should focus on optimising NFC dispersion techniques, including surface modification of NFC, solvent-assisted mixing, ultrasonic dispersion, or the use of compatibilizers to improve interfacial adhesion between NFC and the polymer matrix.

Furthermore, varying NFC loading levels is also vital to identify the optimal reinforcement concentration that maximises mechanical performance without compromising ductility or toughness. Investigations using single-component biopolymers, rather than blended resin systems, would also provide clearer insights into NFC–polymer interactions.

Thus, addressing these aspects is expected to significantly improve NFC yield, material consistency, and composite performance, further strengthening the potential of agricultural waste-derived NFC as a scalable and sustainable reinforcement material for biodegradable polymer applications.

Acknowledgments

The authors gratefully acknowledge the Department of Materials Science and Engineering, Faculty of Engineering and Industrial Technology, Silpakorn University, Thailand, for the facility support. We also greatfully thank NANO ONIONS, Co. Ltd. for financial assitance in this work.

References

[1]. AbouelNour, Y., Rakauskas, N., Naquila, G., & Gupta, N. (2024). Tensile testing data of additive manufactured ASTM D638 standard specimens with embedded internal geometrical features. *Scientific Data*, 11(1), 506. https://doi.org/10.1038/s41597-024-03369-y

[2]. Anderson, J. P., & Altan, M. C. (2015). Formation of voids in composite laminates: Coupled effect of moisture content and processing pressure. *Polymer Composites*, 36(2), 376–384. https://doi.org/10.1002/pc.22952

[3]. Athanasopoulou, E., Barroso, T. L. C. T., & Hernández-García, E. (2026). Seaweed Biomass as a Sustainable Raw Material for Food Packaging: A Review on Biomolecules, Properties, Applications, Limitations and Future Perspectives. *Applied Sciences*, 16(12), 5836. https://doi.org/10.3390/app16125836

[4]. Barkane, A., Jurinovs, M., Starkova, O., Grase, L., Schmidt, D. F., & Gaidukovs, S. (2023). Enhancing Stiffness, Toughness, and Creep in a 3D-Printed Bio-Based Photopolymer Using Ultra-Low Contents of Nanofibrillated Cellulose. *Journal of Composites Science*, 7(10), 435. https://doi.org/10.3390/jcs7100435

[5]. Cabrera-Villamizar, L. A., Ebrahimi, M., Martínez-Abad, A., Talens-Perales, D., López-Rubio, A., & Fabra, M. J. (2024). Order matters: Methods for extracting cellulose from rice straw by coupling alkaline, ozone and enzymatic treatments. *Carbohydrate Polymers*, 328, 121746. https://doi.org/10.1016/j.carbpol.2023.121746

[6]. Coldebella, R., Gentil, M., Berger, C., Dalla Costa, H. W., Pedrazzi, C., Labidi, J., Delucis, R. A., & Missio, A. L. (2021). Nanofibrillated Cellulose-Based Aerogels Functionalized with Tajuva (Maclura tinctoria) Heartwood Extract. *Polymers*, 13(6), 908. https://doi.org/10.3390/polym13060908

[7]. Evode, N., Qamar, S. A., Bilal, M., Barceló, D., & Iqbal, H. M. N. (2021). Plastic waste and its management strategies for environmental sustainability. *Case Studies in Chemical and Environmental Engineering*, 4, 100142. https://doi.org/10.1016/j.cscee.2021.100142

[8]. Fernández-Santos, J., Valls, C., Cusola, O., & Roncero, M. B. (2022). Composites of cellulose nanocrystals in combination with either cellulose nanofibril or carboxymethylcellulose as functional packaging films. *International Journal of Biological Macromolecules*, 211, 218–229. https://doi.org/10.1016/j.ijbiomac.2022.05.049

[9]. Harahap, M., Purwandari, V., Zebua, D. A., Daulay, N., Situmorang, S. A., Perangin Angin, Y. A., Ong, A. J., Siow, J., Goei, R., Tok, A. l. Y., & Gea, S. (2025). Extraction and characterization of cellulose nanofibers from rice husk: Potential for electrospun PVA/CNF mat composites. *Kuwait Journal of Science*, 52(3), 100403. https://doi.org/10.1016/j.kjs.2025.100403

[10]. International, A. (2023). ASTM D256–23: Standard test methods for determining the Izod pendulum impact resistance of plastics. In: ASTM International.

[11]. Javier-Astete, R., Jimenez-Davalos, J., & Zolla, G. (2021). Determination of hemicellulose, cellulose, holocellulose and lignin content using FTIR in Calycophyllum spruceanum (Benth.) K.

Schum. and Guazuma crinita Lam. *PLOS ONE*, 16(10), e0256559. https://doi.org/10.1371/journal.pone.0256559

[12].Jiang, F., Kondo, T., & Hsieh, Y.-L. (2016). Rice Straw Cellulose Nanofibrils via Aqueous Counter Collision and Differential Centrifugation and Their Self-Assembled Structures. *ACS Sustainable Chemistry & Engineering*, 4(3), 1697–1706. https://doi.org/10.1021/acssuschemeng.5b01653

[13].Juan-Cano, M. E., Gonzalez, Z., Rincón, E., Sanchez-Herencia, A. J., Ferrari, B., & Ferrández-Montero, A. (2025). Tuning Biodegradation and Physicochemical Features of PLA/HAp Biomaterials by Incorporating Nanofibrillated Cellulose Through a Colloidal Processing Route. *Polymers*, 17(12), 1595. https://doi.org/10.3390/polym17121595

[14].Jusakulvijit, P., Bezama, A., & Thrän, D. (2021). The Availability and Assessment of Potential Agricultural Residues for the Regional Development of Second-Generation Bioethanol in Thailand. *Waste and Biomass Valorization*, 12(11), 6091–6118. https://doi.org/10.1007/s12649-021-01424-y

[15].Koh, J. J., Zhang, X., & He, C. (2018). Fully biodegradable Poly(lactic acid)/Starch blends: A review of toughening strategies. *Int J Biol Macromol*, 109, 99–113. https://doi.org/10.1016/j.ijbiomac.2017.12.048

[16].Kumar, R., Verma, A., Shome, A., Sinha, R., Sinha, S., Jha, P. K., Kumar, R., Kumar, P., Shubham, Das, S., Sharma, P., & Vara Prasad, P. V. (2021). Impacts of Plastic Pollution on Ecosystem Services, Sustainable Development Goals, and Need to Focus on Circular Economy and Policy Interventions. *Sustainability*, 13(17), 9963. https://doi.org/10.3390/su13179963

[17].Li, X., Chen, J., Liu, J., & Yang, K. (2023). Silane modification of nanofibrillated cellulose and its effect on the properties of waterborne acrylic resin. *Journal of Applied Polymer Science*, 140. https://doi.org/10.1002/app.54543

[18].Li, Z., Lin, Y., Cheng, H., Qian, S., & Fang, X. (2025). Synergistic effects of thermoplastic starch and nanofibrillated cellulose on the mechanical, thermal, and micromorphological properties of polylactic acid composites. *Polymer Composites*, 46(9), 8336–8348. https://doi.org/10.1002/pc.29496

[19].Li, Z., Zhang, Z., Cheng, H., Qian, S., & Liu, Y. (2024). Nanofibrillated cellulose reinforced polypropylene carbonate biocomposites with high mechanical properties, dimensional stability, and antibacterial properties. *Polymer Composites*, 45(12), 11447–11458. https://doi.org/10.1002/pc.28577

[20].Lim, C., Yusoff, S., Ng, C. G., Lim, P. E., & Ching, Y. C. (2021). Bioplastic made from Seaweed Polysaccharides with Green Production Methods. *Journal of Environmental Chemical Engineering*, 9, 105895. https://doi.org/10.1016/j.jece.2021.105895

[21].Liu, P. C., W. Liu, L. (2021). Cellulose nanocrystals: Pretreatments, preparation strategies, and emerging applications. *Carbohydrate Polymers*, 275, 118751. https://doi.org/10.1016/j.carbpol.2021.118751

[22].Mateo, S., Peinado, S., Morillas-Gutiérrez, F., La Rubia, M. D., & Moya, A. J. (2021). Nanocellulose from Agricultural Wastes: Products and Applications—A Review. *Processes*, 9(9), 1594. https://doi.org/10.3390/pr9091594s

[23].Md Salim, R., Asik, J., & Sarjadi, M. S. (2021). Chemical functional groups of extractives, cellulose and lignin extracted from native Leucaena leucocephala bark. *Wood Science and Technology*, 55(2), 295–313. https://doi.org/10.1007/s00226-020-01258-2

[24].Moon, R., Johnston, L., Land-Hensdal, C., & Batchelor, W. (2025). Perspectives on cellulose nanofibril size measurement using scanning electron microscopy. *Cellulose*, 32(5), 2793–2810. https://doi.org/10.1007/s10570-025-06458-2

[25].Nano Onions Co., L. Nano Onions [Internet]. 2023 [updated cited 10 Nov 2025]. Available from: https://nanoonions.co/.

[26].Nofar, M., Sacligil, D., Carreau, P. J., Kamal, M. R., & Heuzey, M. C. (2019). Poly (lactic acid) blends: Processing, properties and applications. *Int J Biol Macromol*, 125, 307–360. https://doi.org/10.1016/j.ijbiomac.2018.12.002

[27].Oriez, V., Peydecastaing, J., & Pontalier, P.-Y. (2020). Lignocellulosic Biomass Mild Alkaline Fractionation and Resulting Extract Purification Processes: Conditions, Yields, and Purities. *Clean Technologies*, 2(1), 91–115.

[28].Platnieks, O., Gaidukovs, S., Barkane, A., Sereda, A., Gaidukova, G., Grase, L., Thakur, V. K., Filipova, I., Fridrihsone, V., Skute, M., & Laka, M. (2020). Bio-Based Poly(butylene succinate)/Microcrystalline Cellulose/Nanofibrillated Cellulose-Based Sustainable Polymer Composites: Thermo-Mechanical and Biodegradation Studies. *Polymers*, 12(7), 1472. https://doi.org/10.3390/polym12071472

[29].Prume, J. A., Gorka, F., & Löder, M. G. J. (2021). From sieve to microscope: An efficient technique for sample transfer in the process of microplastics' quantification. *MethodsX*, 8, 101341. https://doi.org/10.1016/j.mex.2021.101341

[30].Qiao, X., Wang, Z., & Sun, K. (2021). Renewable Rice Straw Cellulose Nanofibril Reinforced Poly (ε-caprolactone) Composite Films. *Research Square PREPRINT (Version* 1) *available at Research Square* https://doi.org/10.21203/rs.3.rs-1169920/v1

[31].Ratnakumar, A., Samarasekara, A. M. P. B., Amarasinghe, D. A. S., & Karunanayake, L. (2021, 27–29 July 2021). Individualization of Nanofibrillated Cellulose from Sri Lankan Rice Straw: Structural Characteristics and Thermal Properties. 2021 Moratuwa Engineering Research Conference (MERCon),

[32].Ruan, L., Wu, H., Wu, S., Zhou, L., Wu, S., & Shang, C. (2024). Optimizing the Conditions of Pretreatment and Enzymatic Hydrolysis of Sugarcane Bagasse for Bioethanol Production. *ACS Omega*, 9(27), 29566–29575. https://doi.org/10.1021/acsomega.4c02485

[33].Samsalee, N., Meerasri, J., & Sothornvit, R. (2023). Rice husk nanocellulose: Extraction by high-pressure homogenization, chemical treatments and characterization. *Carbohydrate Polymer Technologies and Applications*, 6, 100353. https://doi.org/10.1016/j.carpta.2023.100353

[34].Sharma, N., Allardyce, B. J., Rajkhowa, R., & Agrawal, R. (2023). Rice straw-derived cellulose: a comparative study of various pre-treatment technologies and its conversion to nanofibres. *Scientific Reports*, 13(1), 16327. https://doi.org/10.1038/s41598-023-43535-7

[35].Shrestha, S. (2019). *Effect of nanocellulose reinforcement on the properties of polymer composites* Purdue University]. https://doi.org/10.25394/PGS.8039027.v1

[36].Simão, C. D., Reparaz, J. S., Wagner, M. R., Graczykowski, B., Kreuzer, M., Ruiz-Blanco, Y. B., García, Y., Malho, J.-M., Goñi, A. R., Ahopelto, J., & Sotomayor Torres, C. M. (2015). Optical and mechanical properties of nanofibrillated cellulose: Toward a robust platform for next-generation green technologies. *Carbohydrate Polymers*, 126, 40–46. https://doi.org/10.1016/j.carbpol.2015.03.032

[37].Tanpichai, S. (2018). A comparative study of nanofibrillated cellulose and microcrystalline cellulose as reinforcements in all-cellulose composites. *Journal of Metals, Materials and Minerals*, 28(1). https://doi.org/10.14456/jmmm.2018.3

[38].Thangapandian, P., Seenivasan, S., Raj Kumar, P., Kailasavalli, S., & Paulsingarayar, S. (2024). Effects of chemical treatment on natural (rice straw/neem saw dust) fiber morphology and mechanical properties of its composite material. *Materials Letters*, 364, 136288. https://doi.org/10.1016/j.matlet.2024.136288

[39].Thushari, G. G. N., & Senevirathna, J. D. M. (2020). Plastic pollution in the marine environment. *Heliyon*, 6(8), e04709. https://doi.org/10.1016/j.heliyon.2020.e04709

[40].Velázquez, M. E., Ferreiro, O. B., Menezes, D. B., Corrales-Ureña, Y., Vega-Baudrit, J. R., & Rivaldi, J. D. (2022). Nanocellulose Extracted from Paraguayan Residual Agro-Industrial Biomass: Extraction Process, Physicochemical and Morphological Characterization. *Sustainability*, 14(18), 11386. https://doi.org/10.3390/su141811386

[41].Velghe, I., Buffel, B., Cardinaels, R., Vandeginste, V., Thielemans, W., & Desplentere, F. (2024). Quantification of PLA degradation in the melt phase using a parallel plate rheometer. *Polymer Testing*, 137, 108506. https://doi.org/10.1016/j.polymertesting.2024.108506

[42].Wada, M., Okano, T., & Sugiyama, J. (2001). Allomorphs of native crystalline cellulose I evaluated by two equatoriald-spacings. *Journal of Wood Science*, 47(2), 124–128. https://doi.org/10.1007/BF00780560

[43].Widodo, E., Pratikto, Sugiarto, & Widodo, T. D. (2024). Comprehensive investigation of raw and NaOH alkalized sansevieria fiber for enhancing composite reinforcement. *Case Studies in Chemical and Environmental Engineering*, 9, 100546. https://doi.org/10.1016/j.cscee.2023.100546

[44].Yeligbayeva, G., Orazalin, Z. K., Alfergani, A., Omirzakova, K., Milissova, N. B., & Kusrini, E. (2025). Effect of Rice Straw on the Mechanical and Biodegradability Properties of the Poly (Polyethylene-G-Acrylic Acid). *Kompleksnoe ispol'zovanie mineral'nogo syr'â/Complex Use of Mineral Resources/Mineraldik shikisattardy Keshendi Paidalanu*, 338, 51–58. https://doi.org/10.31643/2026/6445.28

[45].Zhang, Y. W., X. Liu, X. (2021). Extraction and characterization of nanocellulose from agricultural residues for composite applications. *Industrial Crops and Products*, 173, 114123. https://doi.org/10.1016/j.indcrop.2021.114123